Coupled 2D/3D Transport: Analysis of Graphene-SiC Devices

M.G. Ancona, K.D. Hobart, and T.J. Anderson
Electronics S&T Division
Naval Research Laboratory
Washington, DC, USA
ancona@estd.nrl.navy.mil

***Abstract*—Macroscopic equations are discussed that describe carrier transport in situations in which an ordinary 3D semiconductor is coupled to a 2D material like graphene or molybdenum disulfide. The transport equations are familiar ones from either diffusion-drift or density-gradient theory, with the main focus being on the critical boundary conditions that couple the two systems together. To illustrate the hybrid description we apply it to situations involving graphene on p-type SiC.**

Keywords—graphene; SiC; diffusion-drift; density-gradient; transport theory.

I. Introduction

The recent advent of materials like graphene, molybdenum disulfide, and silicene has led to an intensive worldwide investigation of electronic and optoelectronic devices in which the carrier transport takes place in a single (or a few) atomic layer(s) and is thus physically constrained to be 2D. Further expanding the opportunities is the possibility of hybrid device designs in which 2D materials are integrated with each other (van der Waals solids) [1] or with ordinary 3D semiconductors [2-4]. To support these prospects, e.g., for photovoltaics [5], device modeling tools are obviously needed. This need seems to be largely addressed for the pure 2D case, with both microscopic [6] and macroscopic [7] approaches and tools being well established. In the present work we therefore focus on the hybrid situations, and especially on the 2D/3D case, building on [7] by further developing the macroscopic modeling approach that tends to have the most value for practical engineering.

In formulating the hybrid 2D/3D theory in Section II we follow [7] in treating the 2D materials using a diffusion-drift description consisting of 2D transport equations plus an electrostatic boundary condition applied across the layer. Likewise we employ standard continuum theories of 3D semiconductor transport, using either conventional diffusion-drift (DD) theory or density-gradient (DG) theory [8], with the latter allowing tunneling effects in the vicinity of the 2D/3D junction to be represented. Of most importance are the coupling boundary conditions, applied at the 2D/3D boundaries and that interrelate the 2D and 3D variables. For concreteness and purposes of illustration we apply the hybrid theory to various device situations involving graphene/SiC junctions that are easily formed, for example, by sublimation of silicon from SiC at high temperature or by CVD/transfer.

II. Theory

The hybrid theory developed herein is macroscopic in character, and so is concerned with populations of charge carriers that are represented by density variables, subject to continuum assumptions, and governed by the laws of classical field theory. Also, for this paper steady-state conditions are assumed throughout.

A. Differential Equations

For the description of bulk semiconductors we use either DD theory or the scattering-dominated "DGC" version of DG theory as discussed in [8]. Written in unified form, the differential equations of these theories are

$$(1a) \qquad \left(\varepsilon_{SiC}\psi_{,i}\right)_{,i} = q(N_A - p + n)$$

$$(1b) \quad \left[\mu_n n \Phi^n_{,i}\right]_{,i} = G - R \qquad \frac{1}{s}\left(b_n s_{,i}\right)_{,i} = \Phi^n - \psi + \varphi^n(n)$$

$$(1c) \quad \left[\mu_p p \Phi^p_{,i}\right]_{,i} = R - G \qquad \frac{1}{r}\left(b_p r_{,i}\right)_{,i} = \Phi^p - \psi - \varphi^p(p)$$

where $s \equiv \sqrt{n}$ and $r \equiv \sqrt{p}$, the DD description results when the DG coefficients b_n and b_p are set to zero, i varies from 1 to 3 to represent the x, y, and z coordinates, the "comma" subscript notation indicates partial differentiation, and the Einstein summation convention is assumed. The functions $\varphi^n(n)$ and $\varphi^p(p)$ are the respective DD electron and hole chemical potentials for which expressions are well known, Φ^n and Φ^p are the respective electron and hole electrochemical potentials, and all other parameters take their usual meanings. For 2D materials we assume DD transport so that the differential equations are [7]:

$$(2a) \qquad \bar{J}^n_{\alpha,\alpha} = \left[\bar{\mu}_n \bar{n}(\psi - \bar{\varphi}^n)_{,\alpha}\right]_{,\alpha} = \bar{R} - \bar{G} - \bar{T}_n$$

$$(2b) \qquad \bar{J}^p_{\alpha,\alpha} = -\left[\bar{\mu}_p \bar{p}(\psi + \bar{\varphi}^p)_{,\alpha}\right]_{,\alpha} = \bar{R} - \bar{G} - \bar{T}_p$$

where over-bars indicate 2D variables, and $\alpha = 1{,}2$ denotes the components of the coordinate system defining positions in the 2D material. Like G and R in (1b) and (1c), $\bar{G}$ in (2a) and (2b) accounts for photogeneration in the 2D material while $\bar{R}$

The authors thank the Office of Naval Research for funding support.

978-1-4673-7860-4/15/$31.00 ©2015 IEEE

is the recombination rate [6,9], and as discussed further below, $\bar{T}_n$ and $\bar{T}_p$ are the respective local net rates of transfer of electrons and holes into the 2D material from neighboring layers. Finally, the electron and hole chemical potentials $\bar{\varphi}^n$ and $\bar{\varphi}^p$ are functions of their corresponding densities with the relationships in the case of graphene being:

$$(3a) \qquad \bar{n}(\bar{\varphi}^n) = \int_0^\infty \frac{N_{cv}\,\varepsilon\,d\varepsilon}{1+exp\left[\varepsilon+\frac{\bar{\varphi}^n-E_{bar}}{kT}\right]}$$

$$(3b) \qquad \bar{p}(\bar{\varphi}^p) = \int_0^\infty \frac{N_{cv}\,\varepsilon\,d\varepsilon}{1+exp\left[-\varepsilon-\frac{\bar{\varphi}^p-E_{bar}}{kT}\right]}$$

where $N_{cv} \cong 9.8\times10^{10}\text{cm}^{-2}$ (at room temperature) and $E_{bar} \equiv E_C(\text{SiC}) - E_{Dirac}(\text{graphene}) \cong 0.5\text{eV}$ is the energy offset between the SiC conduction band and the Dirac point in the graphene [4]. The integrals in (3a) and (3b) can be used as is within the numerical scheme or they can be approximated by simple algebraic expressions [7] or look-up tables.

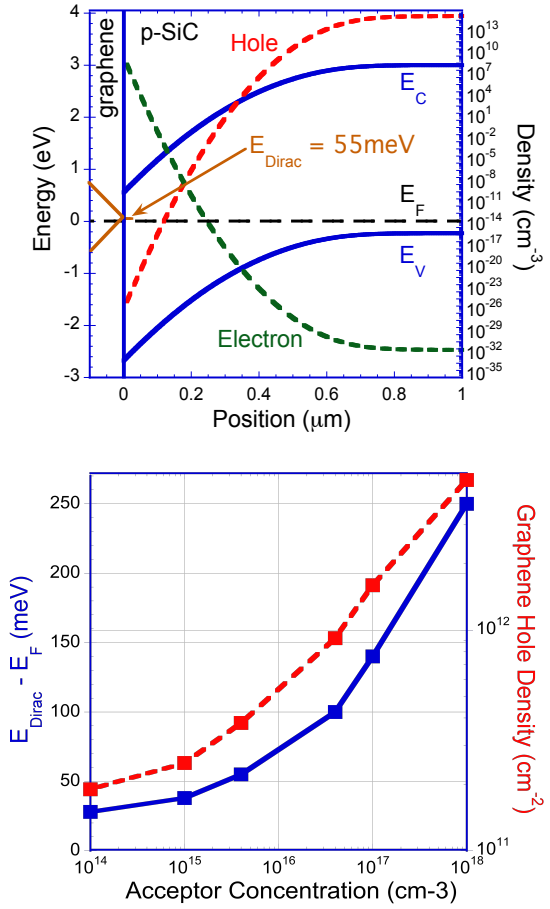

Fig. 1. (a) Band diagram and carrier density profiles for a graphene-p-SiC heterojunction. (b) Simulated graphene Fermi level position and hole density versus SiC doping concentration.

B. Boundary Conditions

As discussed in [7], a first condition that is relevant for any 2D material including when layered or atop a 3D semiconductor is an electrostatic one applied across it:

$$(4a) \qquad \varepsilon_{SiC}\psi_{,3}^{SiC} - \varepsilon_{air}\psi_{,3}^{air} = q(\bar{n}-\bar{p}-\bar{N})$$

where the "3" direction is normal to the layer and the 2D material has been assumed to be interposed between SiC and air.

The crucial set of boundary conditions for the present paper relate to the possibility of interchange of charge between the 2D layer and adjacent materials as expressed in the 2D transport equations (2a) and (2b) through the terms $\bar{T}_n$ and $\bar{T}_p$. When these charge transfers occur into or out of a neighboring 3D semiconductor, then these same terms must enter the boundary conditions, and in particular through charge conservation conditions applied at the interface:

$$(4b) \qquad -J_3^n = \bar{T}_n \qquad -J_3^p = \bar{T}_p$$

One way of viewing these conditions is that the 2D material acts as an "interface trap" analogous to those long studied at semiconductor surfaces. Following this analogy, expressions for $\bar{T}_n$ and $\bar{T}_p$ can then be developed by considering rates of capture and emission.

C. Numerical Methods

To apply the foregoing theory, we formulate boundary value problems appropriate to the devices of interest. In all problems treated herein we assume the variations in the "width" direction can be ignored so that the equations in the 3D semiconductor reduce to 2D and in the 2D material reduce to 1D. The numerical formulations are standard, with the DD version using quasi-Fermi level variables and the DG version using Slotboom-type variables. The solutions are obtained using the Comsol FEM package (see www.comsol.com).

III. Applications

In this section we illustrate the hybrid theory with various 2D/3D device examples in which graphene forms junctions with p-SiC.

A. Equilibrium

When the graphene is itself undoped it will tend to be remotely doped by the nearby acceptors in the p-SiC. But the fact that the graphene's Dirac point is energetically close to the SiC conduction band [2] means this effect will be relatively modest, and unless heavily doped the p-SiC surface will be depleted or weakly inverted. This basic action may be studied in 1D equilibria, with some illustrative solution profiles being depicted in Fig. 1a for a case where the SiC is weakly inverted. The effect of increasing the SiC acceptor concentration on the "doping" of the graphene is shown in Fig. 1b with both the graphene density and Fermi level position being displayed. Finally in Fig. 2 we show the 2D variation in the electric potential potential around a junction formed between SiC and a graphene disk; the same depletion/weak inversion effect of the graphene as seen in Fig. 1a is again apparent.

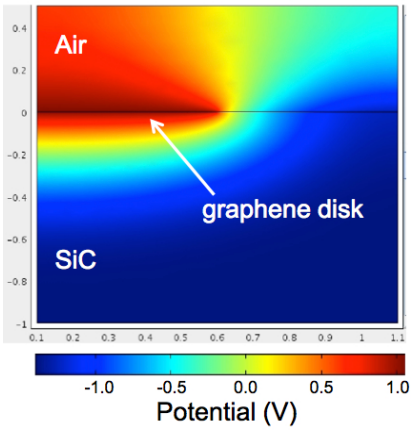

Fig. 2. Electric potential in the vicinity of a graphene disk on the surface of a SiC substrate.

B. Field Termination

The second example we consider is a hypothetical SiC p-n power diode in which, as depicted in Fig. 3, graphene strips or rings are inserted as a novel field termination similar to the concept of [10]. The hope is that the conductive graphene can (via the tangential electrostatic condition) moderate the lateral electric field in the underlying SiC sufficiently to raise the breakdown voltage. Since the graphene strips are not contacted it would seem reasonable to represent them as floating at the unbiased potential, however, simulation finds that the SiC conduction band of the first graphene strip is then pulled below the graphene Fermi energy, meaning that the graphene will ionize and its potential will change. To treat this situation we assume that the graphene strip ionizes to the point

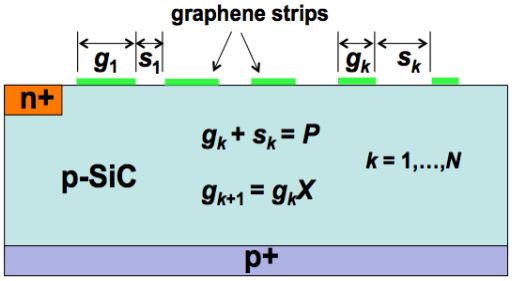

Fig. 3. Graphene field termination design simulated by solving the 2D/3D hybrid equations.

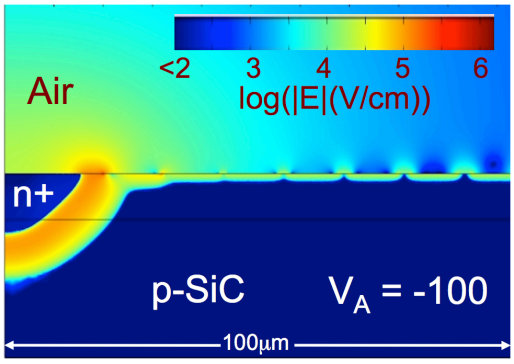

Fig. 4a. The simulated band diagram across the surface when the graphene is assumed to be floating.

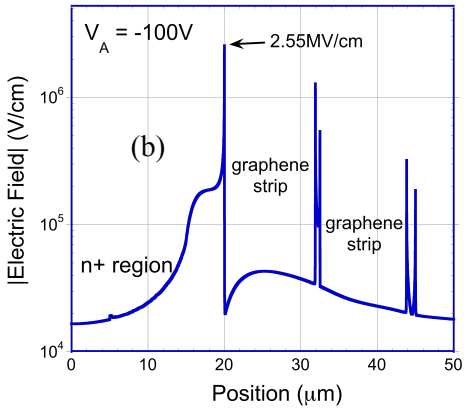

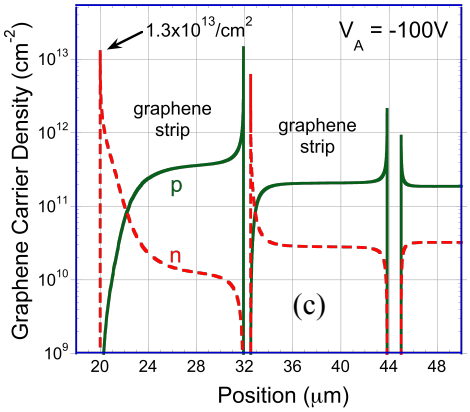

Fig. 4. The simulated (b) electric field and (c) electron and hole densities in the first few graphene strips when the SiC is reverse biased at 100V.

that the Fermi level is pulled just below E_c of the SiC. As illustration, we consider a p-n diode reverse-biased at 100V, and show solution profiles for the electric field and the graphene electron and hole densities in Figs. 4a-c. The strong band-bending seen in the graphene, and the consequent size of the electric field in the first strip (Fig. 4b) at this relatively small voltage (for a power diode) suggest that the single-layer graphene is not conductive enough for this application; whether multi-layer graphene would suffice remains to be explored.

C. Forward Bias

Next we consider an n-graphene/p-SiC junction under forward bias as was studied experimentally in [4]. As suggested by the band diagram in Fig. 1a, the behavior should be current much like that of a Schottky barrier, and dominated by hole injection from the SiC into the graphene. A thermionic DD simulation gives the result shown in Fig. 5 (in blue). Clearly, the calculated threshold voltage and current are higher and the ideality factor is lower than those measured experimentally [4]. A possible explanation is hole tunneling, and to examine this we employ DG theory and find (in red, Fig. 5) that it can indeed be important at graphene edges where the enhanced electric field acts to narrow the barrier. The

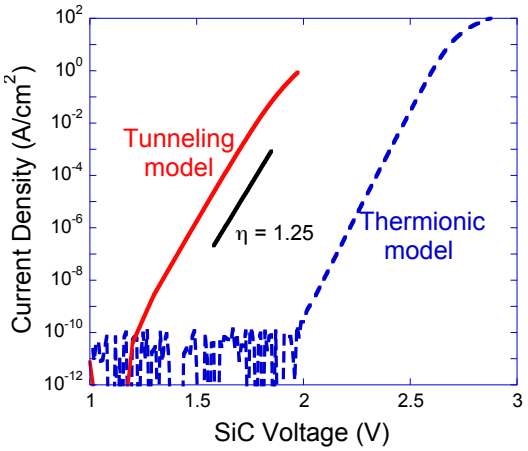

Fig. 5. Comparison between the simulated thermionic current (DD) of a graphene/SiC diode with a thermionic/tunneling (DG) simulation which includes an edge. The latter corresponds better to experiment [4].

threshold voltage and current levels are much closer to experiment [4], however, the ideality factor is still low.

D. Transparent Graphene Contacts

As a final application we consider a graphene/SiC diode under forward bias where the electrical contact to the graphene is restricted to a small area, thus leaving the remainder of the area open, e.g., for photon absorption in a solar cell or photodetector application. For illustration, we use the DD equations to model one half of a symmetric diode structure formed of n-type graphene and p-type SiC in which a 0.2μm wide contact region is set at the center of a 20μm wide region. For a forward bias of 3V, in Fig. 6a we plot the electric potential (in half the symmetric region) and observe it to be significantly non-uniform as a result of the relatively poor conductivity of the graphene. This is seen more directly by the drop-off in current density plotted in Fig. 6b (red curve). Also shown in that figure is the graphene electron and hole densities (blue). Simulations of this type could be used, for example, to design the separation distance between metal contacts in a transparent electrode.

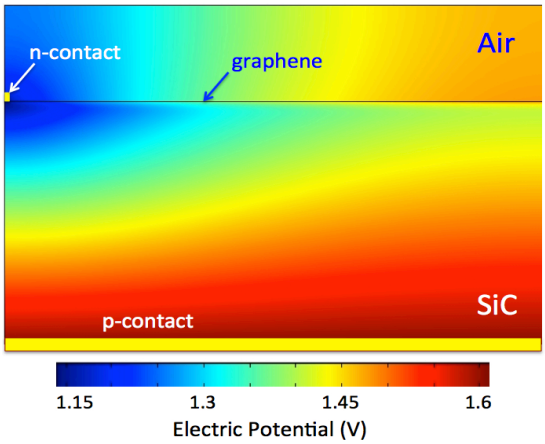

Fig. 6a. The electric potential in an n-graphene/p-SiC diode. The device is symmetrical about the left edge with the SiC region shown being 10μm wide and 1μm thick.

IV. Final Remarks

The results of this paper illustrate the use and value of the 2D/3D hybrid transport theory for a number of technologically relevant device situations. To be most value the theory will require better characterization of the materials involved, and especially of parameters such as the graphene lifetime [9] and the recombination velocity. In addition, further generalizations of the theory will be need to be investigated including for the case when multiple graphene layers are present [7].

Acknowledgment

The authors thank Fritz Kub, Andrew Koehler, and Marko Tadjer for useful discussions.

References

[1] A.K. Geim and I.V. Grigorieva, "Van der Waals heterostructures," *Nature* **499**, 419 (2013).

[2] S. Tongay, M. LeMaitre, X. Miao, B. Gila, B.R. Appleton, and A.F. Hebard, "Rectification at graphene-semiconductor interfaces: Zero-gap semiconductor-based diodes," *Phys. Rev. X* **2**, 011002 (2012).

[3] C.-C. Chen, M. Aykol, C.-C. Chang, A.F.J. Levi and S.B. Cronin, "Graphene-silicon Schottky diodes," *Nano Lett.* **11**, 1863 (2011).

[4] T.J. Anderson, *et al.*, "Investigation of the epitaxial graphene/p-SiC heterojunction," *IEEE Elect. Dev. Lett.* **33**, 1610-1612 (2012).

[5] K.F. Shi, R.R. Hague, L.F. Mao, and Z.L. Lu, "Graphene-sandwiched silicon structures for greatly enhanced un-polarized light absorption," *Optics Comm.* **339**, 47 (2015).

[6] J. Guo, "Modeling of graphene nanoribbon devices," *Nanoscale* **4**, 5538 (2012).

[7] M.G. Ancona, "Electron transport in graphene from a diffusion-drift perspective," *IEEE Trans. Elect. Dev.* **57**, 681-689 (2010).

[8] M.G. Ancona, "Density-gradient theory: A macroscopic approach to quantum confinement and tunneling in semiconductor devices," *J. Comput. Electron.* **10**, 65-97 (2011).

[9] F. Rana *et al.*, "Carrier recombination and generation rates for intravalley and intervalley phonon scattering in graphene," *Phys. Rev. B* **79**, 115447 (2009).

[10] W. Sung E. Van Brunt, B.J. Baliga, and A.Q. Huang, "A new edge termination technique for high voltage devices in 4H-SiC-multiple-floating-zone junction termination extension," *IEEE Elect. Dev. Lett.* **32**, 880 (2011).

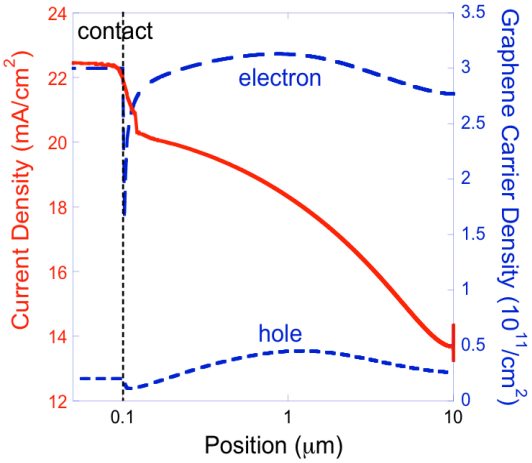

Fig. 6b. Carrier densities and hole injection current in the graphene layer as a function of position.